

Role of Diacylglycerol in PKD Recruitment to the TGN and Protein Transport to the Plasma Membrane

Carole L. Baron and Vivek Malhotra*

Protein kinase D (PKD) is a cytosolic serine-threonine kinase that binds to the trans-Golgi network (TGN) and regulates the fission of transport carriers specifically destined to the cell surface. PKD was found to bind diacylglycerol (DAG), and this binding was necessary for its recruitment to the TGN. Reducing cellular levels of DAG inhibited PKD recruitment and blocked protein transport from the TGN to the cell surface. Thus, a DAG-dependent, PKD-mediated signaling regulates the formation of transport carriers from the TGN in mammalian cells.

PKD contains a cysteine-rich domain (CRD) that comprises two domains (C1a and C1b), a pleckstrin homology (PH) domain, and a kinase domain at the COOH-terminus (1). PKD is recruited to the TGN through Pro¹⁵⁵ of the C1a domain (2), which probably creates a high-affinity binding site for DAG (3). DAG is required for transport of proteins from the Golgi to the cell surface in yeast (4–6). Thus, we sought to test the possibility that PKD-mediated interaction with DAG regulates protein transport to the cell surface by regulating the generation of transport carriers from the TGN in mammalian cells.

We used a protein-lipid overlay assay with NH₂-terminal glutathione S-transferase (GST) fusion proteins (7) to determine the binding of different constructs of PKD to DAG (Fig. 1A). Wild-type PKD, PKD-K618N (a kinase-inactive PKD with Lys⁶¹⁸ changed to Asn), CRD, and C1a domain all bound to DAG. PKD-K618N/P155G (PKD-K618N with a further change of Pro¹⁵⁵ to Gly), GST, and C1b domain, which do not bind to the TGN (2), also did not bind DAG (Fig. 1B). DAG is rapidly turned over in cells (8), thus raising the possibility that PKD might bind additional lipids for its recruitment to the TGN. We thus analyzed the preferential binding of the CRD of PKD to phospholipids adsorbed on nitrocellulose. The CRD bound preferentially to DAG, phosphatidylserine (PS), phosphatidylinositol, and phosphatidylglycerol, but it did not bind to the neutral phospholipids phosphatidylethanolamine and phosphatidylcholine (PC) nor significantly to cholesterol (Fig. 1C). Wild-type PKD, PKD-K618N, and the

C1a domain had the same binding affinity as the CRD. The C1b domain, however, showed no affinity for the lipids tested (9).

Can DAG specifically recruit PKD to lipid membranes? To address this question, we used

1-palmitoyl-2-oleyl-*sn*-glycero-3-phosphocholine (POPC) and POPC/PO-phosphoserine (POPS) liposomes containing increasing concentrations of DAG. The liposomes were incubated with GST-CRD and GST as a negative control. The samples were centrifuged to separate liposome-associated proteins from unbound proteins. The pellets and the supernatants were analyzed by SDS-polyacrylamide gel electrophoresis (PAGE) and Western blotting with polyclonal antibody to GST (anti-GST). We observed more recruitment of the CRD of PKD by POPC in the presence of POPS membranes (Fig. 1, D and E), consistent with the known affinity of PKD for PS (Fig. 1C) (10). However, DAG significantly increased this recruitment, and the binding of CRD to DAG was observed even in the absence of POPS (Fig. 1, D and E). The quantities of wild-type PKD and PKD-K618N recruited to the liposomes also increased in the presence of DAG (9). As expected, GST remained in the supernatant (Fig. 1, D and E, average ratio membrane/cytosolic fraction for GST = 0.65). Thus, DAG could bind and recruit PKD to liposomes.

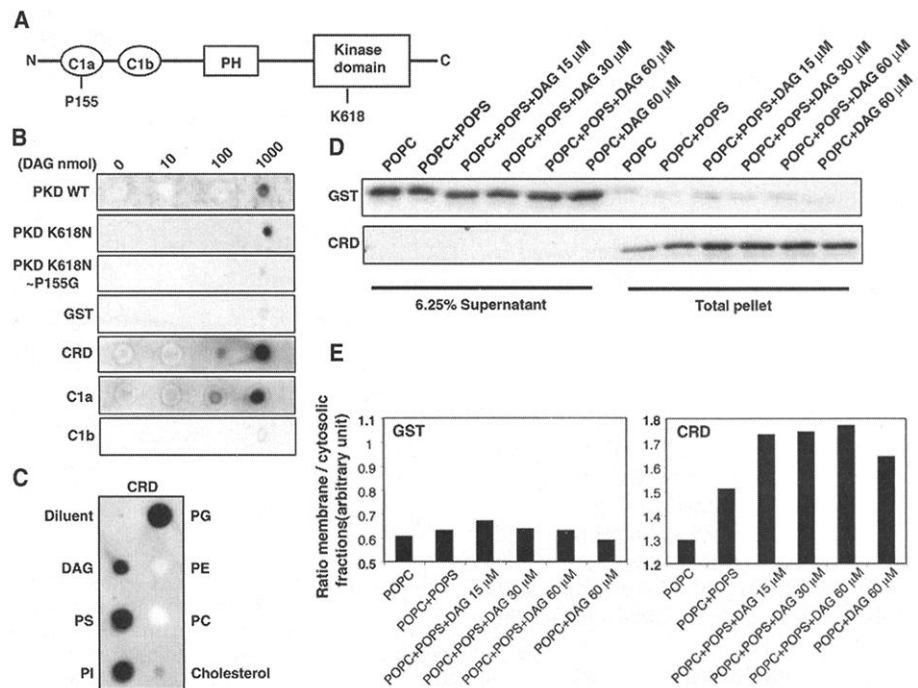


Fig. 1. PKD binds DAG. (A) Schematic representation of the structure of PKD. C1a and C1b, domains of CRD; PH, pleckstrin homology. The ability of the indicated GST fusion proteins (2 μg/ml) to bind DAG (B) or 1000 nmol of different lipids (C) was analyzed by a protein-lipid binding assay on nitrocellulose as described (7). The data are representative of three separate experiments. (D) PKD binding assay was performed by incubating GST or CRD (10 μg/ml) with diC8 that was added to 300 μM POPC or POPC/POPS multilamellar vesicles (molar ratio 4:1) as described (22). Vesicle-bound proteins (pellet) were separated from unbound proteins (supernatant) by high-speed centrifugation and detected by Western blotting with anti-GST. Quantification of the PKD binding was performed with NIH Image software (E). The fusion proteins were expressed in human embryonic kidney 293 cells infected with T antigen of SV40 or in bacteria and purified as instructed by the manufacturer (Amersham Pharmacia Biotech). DAG was purchased from Calbiochem; all other lipids were from Avanti Polar Lipids (Alabaster, Alabama). DAG, diacylglycerol; PS, phosphatidylserine; PI, phosphatidylinositol; PG, phosphatidylglycerol; PE, phosphatidylethanolamine; PC, phosphatidylcholine.

Section of Cell and Developmental Biology, Division of Biology, University of California, San Diego, La Jolla, CA 92093, USA.

*To whom correspondence should be addressed. E-mail: malhotra@biomail.ucsd.edu

REPORTS

To analyze the requirement for DAG in the recruitment of PKD to the TGN, we used two compounds that block DAG production. Fumonisin B1 (FB1) inhibits the ceramide synthase and can thus block the production of DAG and sphingomyelin from ceramide and PC (11–13). Propranolol inhibits the phosphatidic acid (PA) phosphatase (PAP) and thus prevents the dephosphorylation of PA into DAG (14, 15).

HeLa cells stably expressing GST-PKD-K618N were established and described previously (2, 16). These GF17 cells were treated with FB1 for different periods of time. The cellular lipids were extracted to determine the DAG content by a classical DAG kinase assay. This assay shows a decrease in PA production, which is a measure of the decrease in DAG content in the samples treated with FB1. FB1 decreased the DAG content in a time-dependent manner, reaching 30% of the initial level after 24 hours of incubation (Fig. 2A). The effect of FB1 on the localization of GST-PKD-K618N was analyzed by immunofluorescence with anti-GST. In cells treated with FB1, GST-PKD-K618N was predominantly cytosolic (Fig. 2B, upper panels). This treatment did not affect the overall organization of the Golgi apparatus, as revealed by staining with an antibody to the Golgi-specific protein Giantin (Fig. 2B, lower panels). The effect of FB1 on PKD-K618N localization was quantified by homogenization of FB1-treated GF17 cells followed by centrifugation to separate the membrane (pellet) and cytosolic (supernatant) fractions, which were analyzed by SDS-PAGE followed by Western blotting with anti-GST. Cytosolic levels of GST-PKD-K618N doubled upon FB1 treatment (Fig. 2C), consistent with delocalization of GST-PKD-K618N from TGN to the cytosol as observed by immunofluorescence microscopy (Fig. 2B). In a protein-lipid overlay assay with total cellular lipid extracts, CRD and wild-type PKD revealed a marked decrease in binding to lipids extracted from FB1-treated cells relative to controls (Fig. 2D; the best inhibition was seen with 50 μ l of lipid extract). Thus, lowering the DAG levels by FB1 treatment inhibited the binding of PKD to the TGN.

After treatment with propranolol for 5 min, GF17 cells expressing GST-PKD-K618N were analyzed for the Golgi-associated pool of GST-PKD-K618N by fluorescence microscopy with anti-GST. Under these conditions, GST-PKD-K618N was relocated to the cytosol without perturbing the overall organization of the Golgi apparatus (Fig. 3A, compare control and propranolol at 5 min). The effect of propranolol was rapidly reversible, as revealed by the redistribution of GST-PKD-K618N within 5 min of removal of propranolol (Fig. 3A, reversion at 5 min and 1 hour). After 1 hour of propranolol re-

moval, most of the cellular GST-PKD-K618N was localized to the TGN (16). These results show that inhibiting the synthesis of DAG from PA caused a reversible relocation of PKD from the TGN to the cytosol.

To further strengthen the role of DAG in controlling the localization of cellular PKD, we used a cell-permeant analog of DAG called diC8 (1,2-dioctanoyl-*sn*-glycerol). After it inserts into the plasma membrane, diC8 undergoes partitioning across this membrane and into the intracellular membranes (17–19). GF17 cells were incubated with diC8 for 5 or 10 min, and GST-PKD-K618N localization was visualized by fluorescence microscopy with anti-GST. Under these conditions, GST-PKD-K618N was found at the plasma membrane, which is the initial site of diC8 accu-

mulation (Fig. 3B). Upon removal of diC8, the GST-PKD-K618N progressively redistributed to the TGN (Fig. 3B, reversion at 5 to 60 min). Thus, localization of PKD in vivo is regulated by the local concentration of DAG.

It is known that DAG activates PKC ϵ and PKC η and that these kinases in turn activate PKD in vitro (20). Inhibition of PKC activity by specific kinase inhibitors, however, did not affect the localization of PKD-K618N on the Golgi apparatus (9). Thus, the effects of FB1 and propranolol on PKD distribution are not likely to be mediated by an inhibition of PKC ϵ and PKC η (or even other isoforms of the PKC family) but are more likely to occur through a direct inhibition of the interaction of DAG with PKD.

As previously shown, PKD is required for

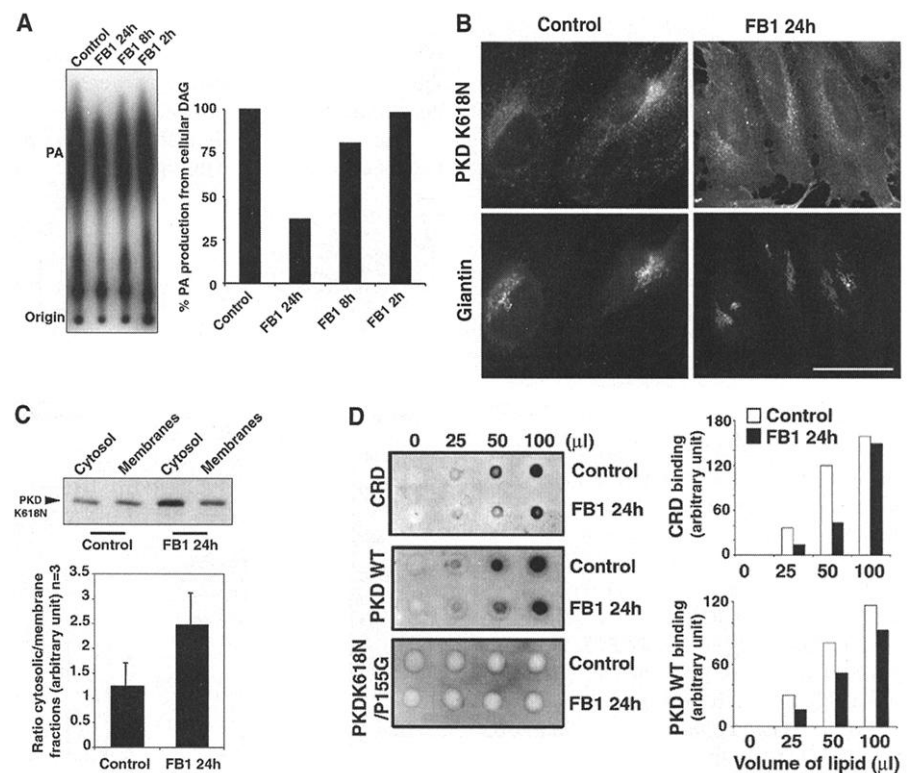


Fig. 2. Regulation of DAG level and PKD-K618N localization by FB1. (A) GF17 cells that stably express GST-PKD-K618N were incubated for 2, 8, or 24 hours with FB1 (25 μ g/ml, Sigma). Total lipid extracts were recovered and DAG content was quantified with a DAG kinase assay in the presence of [γ - 32 P]adenosine triphosphate and thin-layer chromatography according to manufacturer's instructions (Biotrak, DAG assay reagent system kit, Amersham Pharmacia Biotech). Phosphatidic acid (PA) level reflects the quantity of DAG in each sample. Radioactivity was quantified with phosphoimaging and NIH Image software. The data are representative of two different experiments. (B) GF17 cells were incubated for 24 hours with or without FB1 and processed for fluorescence microscopy. GST-PKD-K618N was localized with anti-GST; the organization of the Golgi apparatus was visualized with an antibody to the Golgi-specific protein Giantin. Scale bar, 10 μ m. (C) GF17 cells were incubated with or without FB1 for 24 hours. The cells were recovered by trypsin treatment, washed, homogenized, and fractionated by high-speed centrifugation into membrane (pellet) and cytosol (supernatant) fractions as described (2). The distribution of GST-PKD-K618N was determined by analyzing the pellet and the supernatant by SDS-PAGE and Western blotting with anti-GST. The quantification of three different Western blots is shown in the lower panel. (D) GF17 cells treated with or without FB1 for 24 hours were detached with trypsin and total lipids extracted by the method of Bligh and Dyer (23). Increasing volumes (0 to 100 μ l) of lipids were spotted on nitrocellulose and incubated with GST-tagged CRD, wild-type PKD, and PKD-K618N/P155G. The results were quantified with NIH Image software. The results shown are representative of two different experiments.

REPORTS

protein transport from the TGN to the plasma membrane (16). Depletion of DAG should then inhibit this transport event because of a failure in the recruitment of PKD to the TGN. To test this idea, we infected HeLa cells with the ts045 strain of vesicular stomatitis virus (VSV) as described (21). At 40°C, VSV-G

protein is synthesized but retained in the endoplasmic reticulum (ER) because of a folding defect (Fig. 4A). Upon shifting the cells to 32°C, the VSV-G protein folds and is transported to the Golgi apparatus and then to the cell surface within 60 min (Fig. 4A). In cells pretreated with FB1 for 24 hours, the

VSV-G protein was synthesized and accumulated in the ER at 40°C. Upon shifting the cells to 32°C, the VSV-G protein was transported to the Golgi apparatus. However, its transport from the Golgi to the plasma membrane was delayed and no VSV-G staining was detected at the cell surface even after 2

Fig. 3. DAG regulates the cellular localization of PKD. **(A)** GF17 cells were incubated for 5 min with 500 μ M propranolol (Calbiochem) (22) and either fixed or washed and incubated for 5 or 60 min in complete medium before fixation. The cells were then processed for immunofluorescence microscopy with anti-GST to visualize GST-PKD-K618N, and with antibody to Giantin to monitor the overall organization of the Golgi apparatus. **(B)** GF17 cells were incubated for 5 or 10 min with 25 μ M diC8 (18) and either fixed or washed and incubated for 5, 30, or 60 min in complete medium before fixation. The cells were processed for immunofluorescence microscopy with anti-GST to visualize GST-PKD-K618N. The data are representative of three different experiments. Scale bars, 10 μ m.

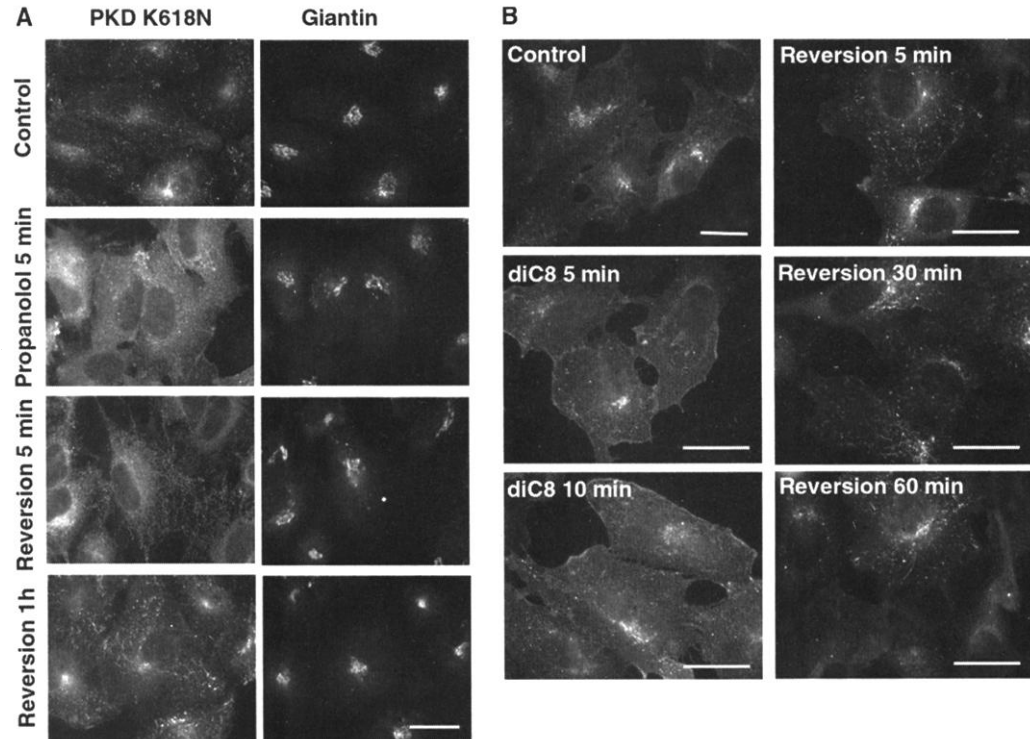
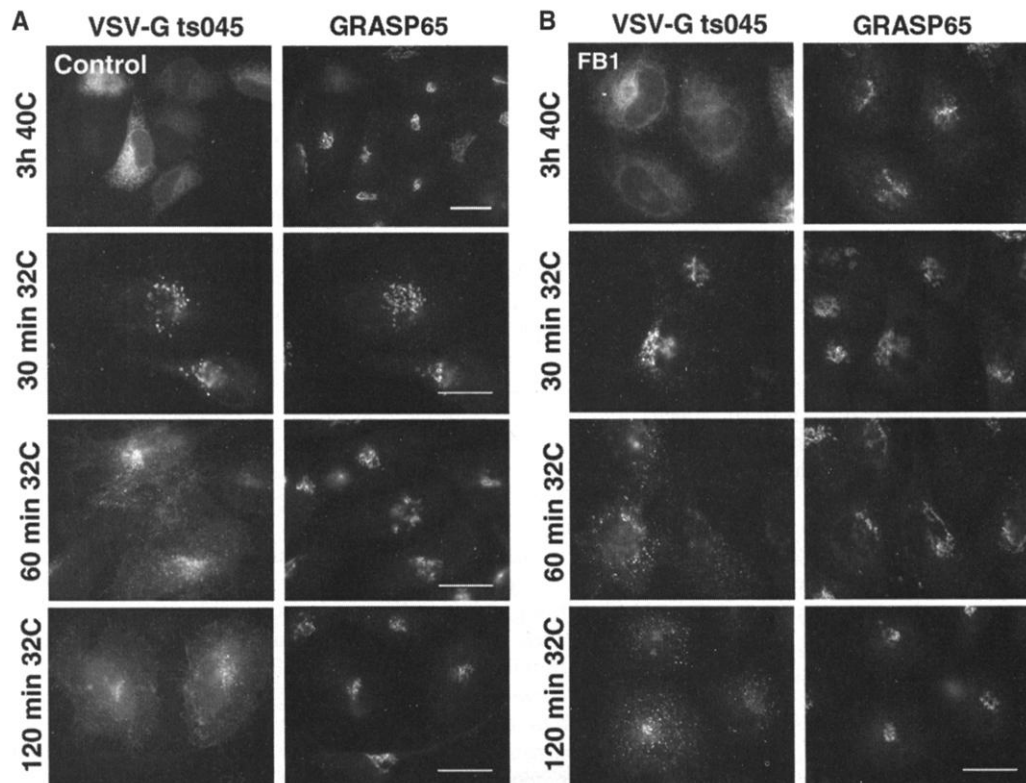


Fig. 4. Regulation of transport from TGN to plasma membrane by DAG. Untreated HeLa cells [(A), control] or HeLa cells treated with FB1 for 24 hours [(B), FB1] were infected with the ts045 strain of VSV and kept at 40°C for 3 hours to accumulate VSV-G proteins in the ER, as described (16). The cells were then incubated at 32°C for different periods of time in the presence of cycloheximide (100 μ g/ml) to permit the transport of VSV-G from the ER along the secretory pathway. The cells were fixed and processed for immunofluorescence microscopy with antibodies to VSV-G and the Golgi-associated protein GRASP65. The data are representative of four different experiments. Scale bars, 10 μ m.



hours at 32°C (Fig. 4B; note the appearance of VSV-G staining at the cell surface after 60 min only in control cells). Therefore, DAG was required for transport of proteins from the TGN to the cell surface.

Our findings reveal that DAG is required for the recruitment of PKD to the TGN and in the stages leading to the formation of transport carriers in mammalian cells. The obvious challenge now is to determine how DAG is generated in the TGN and how its levels are regulated during protein transport specifically from the TGN to the plasma membrane.

References and Notes

1. A. M. Valverde, J. Sinnett-Smith, J. Van Lint, E. Rozengurt, *Proc. Natl. Acad. Sci. U.S.A.* **91**, 8572 (1994).
 2. Y. Maeda, J. V. Van Lint, V. Malhotra, *EMBO J.* **20**, 5982 (2001).

3. G. Zhang, M. G. Kazanietz, P. M. Blumberg, J. H. Hurley, *Cell* **81**, 917 (1995).
 4. B. G. Kearns *et al.*, *Nature* **387**, 101 (1997).
 5. S. E. Phillips *et al.*, *Mol. Cell* **4**, 187 (1999).
 6. R. P. Huijbregts, A. I. de Kroon, B. de Kruijff, *Biochim. Biophys. Acta* **1469**, 43 (2000).
 7. S. Dowler *et al.*, *Biochem. J.* **351**, 19 (2000).
 8. J. Florin-Christensen, M. Florin-Christensen, J. M. Delfino, T. Stegmann, H. Rasmussen, *J. Biol. Chem.* **267**, 14783 (1992).
 9. C. L. Baron, V. Malhotra, data not shown.
 10. A. C. Newton, *Annu. Rev. Biophys. Biomol. Struct.* **22**, 1 (1993).
 11. E. Wang, W. P. Norred, C. W. Bacon, R. T. Riley, A. H. Merrill Jr., *J. Biol. Chem.* **266**, 14486 (1991).
 12. A. H. Merrill Jr., G. van Echten, E. Wang, K. Sandhoff, *J. Biol. Chem.* **268**, 27299 (1993).
 13. W. I. Wu *et al.*, *J. Biol. Chem.* **270**, 13171 (1995).
 14. C. H. Cheng, E. D. Saggerson, *FEBS Lett.* **93**, 120 (1978).
 15. A. S. Pappu, G. Hauser, *Neurochem. Res.* **8**, 1565 (1983).
 16. M. Liljedahl *et al.*, *Cell* **104**, 409 (2001).

17. P. M. Conn *et al.*, *Biochem. Biophys. Res. Commun.* **126**, 532 (1985).
 18. R. J. Davis, B. R. Ganong, R. M. Bell, M. P. Czech, *J. Biol. Chem.* **260**, 1562 (1985).
 19. E. G. Lapetina, B. Reep, B. R. Ganong, R. M. Bell, *J. Biol. Chem.* **260**, 1358 (1985).
 20. J. L. Zugaza, J. Sinnett-Smith, J. Van Lint, E. Rozengurt, *EMBO J.* **15**, 6220 (1996).
 21. G. Griffiths, S. Pfeiffer, K. Simons, K. Matlin, *J. Cell Biol.* **101**, 949 (1985).
 22. P. Sanchez-Pinera, V. Micol, S. Corbalan-Garcia, J. C. Gomez-Fernandez, *Biochem. J.* **337**, 387 (1999).
 23. E. G. Bligh, W. J. Dyer, *Can. J. Biochem. Physiol.* **31**, 911 (1959).
 24. All antibodies and reagents originate as described (2, 16) unless otherwise mentioned. We thank members of the Malhotra laboratory for useful discussions. Supported by a fellowship from ARC, Paris, France (C.L.B.), and by NIH grants GM46224 and GM53747 (V.M.).

2 October 2001; accepted 6 November 2001
 Published online 29 November 2001;
 10.1126/science.1066759
 Include this information when citing this paper.

Identification of a Major Gene Regulating Complex Social Behavior

Michael J. B. Krieger* and Kenneth G. Ross

Colony queen number, a major feature of social organization in fire ants, is associated with worker genotypes at the gene *Gp-9*. We sequenced *Gp-9* and found that it encodes a pheromone-binding protein, a crucial molecular component in chemical recognition of conspecifics. This suggests that differences in worker *Gp-9* genotypes between social forms may cause differences in workers' abilities to recognize queens and regulate their numbers. Analyses of sequence evolution indicate that regulation of social organization by *Gp-9* is conserved in South American fire ant species exhibiting social polymorphism and suggest that positive selection has driven the divergence between the alleles associated with alternate social organizations. This study demonstrates that single genes of major effect can underlie the expression of complex behaviors important in social evolution.

The evolution of complex social behavior is among the most important events in the history of life (1). Interest in the genes underlying the expression of key social traits is strong because knowledge of the genetic architecture will lead to increasingly realistic models of social evolution, while identification of the products of major genes can elucidate the molecular bases of social behavior (2). Few studies have succeeded in showing that complex social behaviors have a heritable basis, and fewer still have suggested that variation in these behaviors is attributable to the action of one or few genes of major effect (3, 4). No candidate genes with major effects on key social polymorphisms have been identified previously.

The fire ant *Solenopsis invicta* displays a fundamental social polymorphism that appears to be under simple genetic control (5, 6). A basic feature of colony social organization, the number of egg-laying queens, is associated with variation at the gene *Gp-9*. In the United States, where this species has been introduced, colonies composed of workers bearing only the *B* allele at *Gp-9* invariably have a single queen (monogyne social form), whereas colonies with workers bearing the alternate, *b* allele have multiple queens (polygyne form) (4). The two social forms differ in many key reproductive and life history characteristics (7), so that the presence of the *b* allele in a colony of workers with the *b* allele induces a fundamental and far-reaching shift in the social system of this ant. Variation at *Gp-9* has been assessed by starch-gel protein electrophoresis (SGPE) coupled with nonspecific protein staining; thus, the gene product and the mechanisms by which it may

influence social behavior were unknown.

We determined the amino acid sequences of several peptide fragments of the GP-9 protein by Edman degradation (8). Degenerate deoxyinosine-oligonucleotide primers (9) corresponding to the NH₂-terminus and an internal peptide fragment were used to amplify the cDNA recovered from reverse transcription of mRNA (10). The amplified fragments were cloned and sequenced. The partial nucleotide sequences of the transcripts then were used to design nondegenerate primers for recovering the full-length mRNA transcripts with a 5' and 3' rapid amplification of cDNA ends approach (5' and 3' RACE) (11). The cap site of *Gp-9* was identified, and its full-length cDNA was found to be 672 base pairs (bp) in length, excluding the polyadenylate tail. The transcript contains an open reading frame of 459 bp, encoding a precursor protein of 153 amino acids (Fig. 1). The mature GP-9 protein, when cleaved of its 19-residue signal peptide (12), has an estimated molecular mass of 14.7 kD. Amplification and sequencing of genomic DNA revealed that the *Gp-9* gene is 1700 bp in length, containing five exons and four introns (Fig. 1A).

GenBank BLASTX searches revealed that *Gp-9* most closely resembles genes encoding moth pheromone-binding proteins (PBPs). Although the amino acid sequence identity is modest (26%), PBPs from different moth species generally have low identity (13), and the size and structure of GP-9 coincide with the consensus characteristics of proteins of this class. Importantly, GP-9 shares with all other PBPs six characteristically spaced cysteine residues (Fig. 1, B and C) (14). Insect PBPs are crucial molecular components in the process of chemical recognition of conspecifics, acting to transport odorant molecules from cuticular pores to receptors on sensory neurons in chemosensilla (15). So-

Department of Entomology, University of Georgia, Athens, GA 30602-2603, USA.

*To whom correspondence should be addressed. E-mail: mkrieger@arches.uga.edu